

STT Analysis of the Time-Dependent Reflected Field From a Moving Dielectric–Magnetic Planar Discontinuity

Timor Melamed, *Senior Member, IEEE*, and Tatiana Danov

Abstract—This paper is concerned with obtaining closed-form exact solution for the 2-D canonical problem of the reflected field from a moving planar discontinuity of a dielectric–magnetic medium that is excited by an impulsive line current. The spectral theory of transient (STT) that originally deals with nondispersive frequency-domain plane-wave spectra is used in this paper for addressing a time-variant scattering problem. The scattering from a moving object yields dispersive and anisotropic PW spectra. Nevertheless, we demonstrate that the STT is capable of dealing with these types of spectra and obtain the desired exact time-dependent solutions. The unique wave phenomena that are associated with the medium and scatterer velocity are explored.

Index Terms—Electromagnetic reflection, Green’s function methods, time-dependent (TD) plane-wave (PW) spectrum.

I. INTRODUCTION

A. Background

PLANE-WAVE (PW) decomposition of time-dependent (TD) fields has been an important tool for the analysis and synthesis of various electromagnetic scattering and diffraction problems [1]. Such spectral representations were used for solving the problem of pulse propagation in dispersive media [2], [3], for antennas and sources characterization [4]–[7], for pulsed-beam decomposition of aperture fields [8], [9], and many more [10]–[13].

The spectral theory of transient (STT) [14]–[16] deals with the explicit description of nondispersive wave processes in the time domain. Under the framework of the STT, the field is expressed as a continuous directional spectrum of nondispersive time-harmonic (TH) PWs, which can be inverted in closed form into the time domain to yield a TD spectral representation. By exploiting its analytic properties, the TD spectral integral can be evaluated in terms of its TD singularities in the complex spectral plane and yields a closed-form solution.

This method has been applied for solving the scattering of pulsed cylindrical wave [16] and pulsed beam [17] from a planar dielectric discontinuity, for pulsed-beams scattering from wedges [18], for the synthesis of short-pulse 2-D wavefields in waveguides [19], and for analyzing the TD PW spectrum of the complex-source pulsed beam [20] and of the airy pulsed beam [21].

Manuscript received April 25, 2017; revised July 2, 2017; accepted July 25, 2017. Date of publication August 2, 2017; date of current version October 5, 2017. (*Corresponding author: Timor Melamed.*)

The authors are with the Department of Electrical and Computer Engineering, Ben-Gurion University of the Negev, Beer Sheva 8499000, Israel (e-mail: timormel@bgu.ac.il).

Color versions of one or more of the figures in this paper are available online at <http://ieeexplore.ieee.org>.

Digital Object Identifier 10.1109/TAP.2017.2734945

Scattering from moving objects is of fundamental importance in antenna and scattering theory, cellular and satellite communication, radar applications, and remote sensing. Though impressive advances have been made in this field, little effort has been made to adjust basic stationary wave theories (such as the geometrical theory of diffraction direct time-domain methods, and the STT) to the scatterer dynamics. In this paper, we examine the possibility to apply the STT procedure for 2-D problem of the incident and reflected fields from a fast moving planar lossless dielectric–magnetic discontinuity due to an impulsive line current. The corresponding *stationary* medium problem is considered as a canonical one since it yields exact closed-form solution, as well as revealing unique and important wave phenomenon, i.e., the lateral (head) wave. Thus, it is of importance to solve the corresponding moving medium problem.

The PW spectra of scattered fields from moving objects in fast motion consist of dispersive and anisotropic PWs. For the best knowledge of the authors, this paper is a first attempt at adjusting the STT that was originally presented for the inversion of TH spectral representations in time-invariant (stationary) scatterers to scattering from moving objects. Specifically, we apply here the PW spectral representations of the relativistic EM TD dyadic Green’s functions of a uniformly moving dielectric–magnetic planar discontinuity that were obtained in [22] and [23]. The spectral representations of the incident and reflected fields under TH excitation are used in this paper in order to obtain closed-form solutions for the corresponding TD EM fields that are excited by an impulsive line current. We explore basic wave phenomena such as the TD local interaction of the incident field with the moving media, the excitation mechanism of the lateral wave, and its canonical form.

The constitutive relations in the medium frame are linear dielectric–magnetic [*vide infra* (4)] over the entire (infinite) frequency band, as in [16], [17], and many others. Though these constitutive relations are valid only in a specific frequency band pending on the materials in question, the resulting fields are considered as an accurate and useful tool for evaluating the EM fields due to TD *volume sources* as long as they are convolved with an appropriate band-limited source.

B. Statement of the Problem

This paper aims at obtaining a closed-form solution for the TD EM incident and reflected fields due to an impulsive line current that is embedded in a uniformly moving dielectric–magnetic medium with a planar discontinuity. Under the

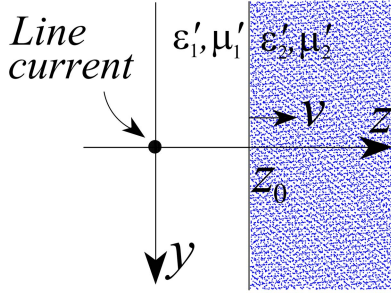


Fig. 1. Physical configuration. An impulsive line current is embedded in a dielectric–magnetic medium with a planar discontinuity. The medium is uniformly moving in speed v in the z -direction. The discontinuity is located in $z = z_0$ at $t = 0$.

framework of special relativity, a 3-D (space–time) event (y, z, ct) in the so-called laboratory frame (here—the source frame) is mapped to the event (y', z', ct') in a comoving frame (the medium frame) by the Lorentz transformation (LT). For a medium-frame velocity of $\mathbf{v} = v\hat{z}$, the LT is given by

$$y' = y, \quad z' = \gamma(z - \beta ct), \quad ct' = \gamma(ct - \beta z) \quad (1)$$

where $c = 1/\sqrt{\epsilon_0\mu_0}$ is the speed of light in vacuum and

$$\beta = v/c, \quad \gamma = 1/\sqrt{1 - \beta^2}. \quad (2)$$

Here and henceforth all physical quantities in the medium frame are denoted by a prime. Unit vectors in the conventional Cartesian coordinate system, (x, y, z) , are denoted by hat over bold fonts. The EM field transformation that is corresponding to $\mathbf{v} = v\hat{z}$ is given in [23]. In this paper, the evaluation of the TD EM fields is carried out *directly* in the source frame. We use the medium frame only for defining the problem and for giving physical interpretations.

The source is an impulsive line current

$$\mathbf{J}(\mathbf{r}, t) = I_0\delta(z)\delta(y)\delta(t)\hat{\mathbf{x}} \quad (3)$$

that is embedded in a uniformly moving dielectric–magnetic medium with a planar discontinuity (see Fig. 1). In the source frame, the medium is moving in a constant translation velocity in the direction of the z -axis.

The medium's discontinuity is located at $z = z_0 > 0$ at time $t = 0$. We assume that the medium is lossless and dispersion free. The constitutive relations in medium frame are given by

$$\begin{aligned} \mathbf{D}'_{1,2}(\mathbf{r}', t') &= \epsilon_0\epsilon'_{r_{1,2}}\mathbf{E}'_{1,2}(\mathbf{r}', t') \\ \mathbf{B}'_{1,2}(\mathbf{r}', t') &= \mu_0\mu'_{r_{1,2}}\mathbf{H}'_{1,2}(\mathbf{r}', t') \end{aligned} \quad (4)$$

where subscripts 1,2 denote fields in $z \leq z'_0$ half space with $z'_0 = \gamma z_0$ denoting the interface location in medium frame [which is obtained from LT in (1)]. The medium in the source frame is bianisotropic and its corresponding constitutive relations are given in [22]. We assume that the medium speed, v , does not exceed either of the medium-frame phase speeds of $c/n'_{1,2}$ where $n'_{1,2}$ are the indices of refraction

$$n'_{1,2} = \sqrt{\epsilon'_{r_{1,2}}\mu'_{r_{1,2}}}. \quad (5)$$

Note that in (3) we assume that the source is located in $z = 0$ and is excited at $t = 0$, whereas the solution

for a generic 2-D TD current density, $J(\mathbf{r}, t)\hat{\mathbf{x}}$, requires a convolution integral for all locations and delays. Nevertheless, the general case solution can be obtained from the $t = 0$ one by an appropriate calibration of the interface location Z_0 .

C. Spectral Theory of Transients

In this section, we briefly review the STT that enables the evaluation of TD fields from the PW spectral synthesis of the corresponding TH fields. We assume a time dependence of $\exp(j\omega t)$ that is denoted by the argument $u(\mathbf{r}, \omega)$. The synthesis of the TH fields by nondispersive local PWs is in the generic form [14]

$$u(\mathbf{r}, \omega) = (j\omega)^{M/2} \frac{-j}{2\pi} \int_{C_N} d^N\kappa \tilde{A}(\mathbf{r}; \kappa) \exp[-j\omega\tilde{\tau}(\mathbf{r}; \kappa)] \quad (6)$$

where \mathbf{r} is the observation point location and $\kappa = (\kappa_1, \kappa_2, \dots)$ are spectral variables that characterize the PW field $\tilde{A}(\mathbf{r}; \kappa) \exp[j\omega\tilde{\tau}(\mathbf{r}; \kappa)]$ with amplitude \tilde{A} and phase $\omega\tilde{\tau}$. M is some integer and N is the dimensionality of the propagating process (i.e., $N = 1$ or 2 for 2-D or 3-D problems, respectively). Here and throughout we denote spectral (κ dependent) constituents by an over tilde. In this paper, we have altered the original $\exp(-i\omega t)$ time dependence of the TH field that was assumed in [14] to $\exp(j\omega t)$ and introduce in this section the corresponding modifications.

The integral in (6) is inverted in closed form into the time domain via the analytic (one-sided) Fourier transform

$$\check{u}(\mathbf{r}, t) = \frac{1}{\pi} \int_0^\infty d\omega u(\mathbf{r}, \omega) \exp(j\omega t), \quad \text{Im } t \geq 0 \quad (7)$$

where we denote analytic fields by the brave sign. The integral in (7) yields an analytic function in the upper $\text{Im } t \geq 0$ plane. Note that though the physical time is real, the *time argument* of an analytic field can be complex [see the evanescent spectral range in (17) where κ_z is complex].

Next we examine the special case of $N = 1$ and $M = 2$, which corresponds to the specific fields in question [*vide infra* (10)]. By denoting the spectral variable as κ_y and applying (7) to (6), the canonical TD spectral integral is given by

$$\check{u}(\mathbf{r}, t) = \frac{\partial_t}{2\pi^2} \int_{C_N} \frac{\tilde{A}(\mathbf{r}; \kappa_y)}{t - \tilde{\tau}(\mathbf{r}; \kappa_y)} d\kappa_y, \quad \text{Im } t \geq 0. \quad (8)$$

The transient integral in (8) can be evaluated in terms of the singularities of the integrand. These are the TD pole singularities $\kappa_y(t)$ that are defined by $\tilde{\tau}[\kappa_y(t)] = t$, $\text{Im } t \geq 0$, and the singularities of $\tilde{\tau}(\kappa_y)$ and $\tilde{A}(\kappa_y)$. For $\tilde{\tau}(\kappa_y)$, these include real branch points $\pm\kappa_{yc}$ at the edges of the propagating (visible) spectrum. For $\tilde{A}(\kappa_y)$, one may have branch points κ_{yb} that are introduced into the visible spectrum by certain interface reflection phenomena in a piecewise continuous medium. Specific examples can be found in [16].

II. TD SPECTRAL REPRESENTATIONS

In this section, we derive the TD *spectral* representations of the incident and reflected fields in the canonical form of (8).

A. Incident Field

The incident EM field is the field that is radiated by the current line source in (3). The source is embedded in a uniformly moving dielectric–magnetic medium of (medium frame) permittivity and permeability of ϵ'_1 and μ'_1 , respectively (for all \mathbf{r}). The analytic signal representation of the EM TD incident field is given by

$$\begin{aligned}\check{\mathbf{E}}^i(\mathbf{r}, t) &= \frac{1}{\pi} \int_0^\infty d\omega \mathbf{E}^i(\mathbf{r}, \omega) \exp(j\omega t), \quad \text{Im } t \geq 0 \\ \check{\mathbf{H}}^i(\mathbf{r}, t) &= \frac{1}{\pi} \int_0^\infty d\omega \mathbf{H}^i(\mathbf{r}, \omega) \exp(j\omega t), \quad \text{Im } t \geq 0\end{aligned}\quad (9)$$

where

$$\begin{aligned}\mathbf{E}^i(\mathbf{r}, \omega) &= \frac{1}{2\pi} \int d\kappa_y \check{\mathbf{E}}^i(\mathbf{r}, \omega; \kappa_y) \\ \mathbf{H}^i(\mathbf{r}, \omega) &= \frac{1}{2\pi} \int d\kappa_y \check{\mathbf{H}}^i(\mathbf{r}, \omega; \kappa_y).\end{aligned}\quad (10)$$

Here $\check{\mathbf{E}}^i(\mathbf{r}, t)$ and $\check{\mathbf{H}}^i(\mathbf{r}, t)$ denote the analytic signals that are corresponding to the real physical signals $\mathbf{E}^i(\mathbf{r}, t)$ and $\mathbf{H}^i(\mathbf{r}, t)$ with frequency spectra $\mathbf{E}^i(\mathbf{r}, \omega)$ and $\mathbf{H}^i(\mathbf{r}, \omega)$.

The integrals in (9) define analytic functions in the upper half of the complex t -plane. The TH spectral PWs, $\check{\mathbf{E}}^i(\mathbf{r}, \omega; \kappa_y)$ and $\check{\mathbf{H}}^i(\mathbf{r}, \omega; \kappa_y)$, were investigated in [22], and were found to be

$$\begin{aligned}\check{\mathbf{E}}^i(\mathbf{r}, \omega; \kappa_y) &= \check{E}_x^i(\mathbf{r}, \omega; \kappa_y) \hat{\mathbf{x}} \\ \check{E}_x^i(\mathbf{r}, \omega; \kappa_y) &= -\frac{I_0 \omega \mu'_1 \sqrt{\alpha}}{2\kappa_z} \exp[-j\omega \tilde{\tau}^i(\kappa_y)]\end{aligned}\quad (11)$$

where

$$\tilde{\tau}^i(\kappa_y) = (\sqrt{\alpha} n'_1 \kappa_y y + \alpha n'_1 \kappa_z z - mz)/c \quad (12)$$

with

$$m = \beta \frac{n_1'^2 - 1}{1 - n_1'^2 \beta^2}, \quad \alpha = \frac{1 - \beta^2}{1 - n_1'^2 \beta^2} \quad (13)$$

denotes the spectral delay of the incident field and

$$\kappa_z = \sqrt{1 - \kappa_y^2}, \quad \text{Re} \kappa_z \geq 0, \quad \text{Im} \kappa_z \leq 0 \quad (14)$$

is the longitudinal (normalized) wavenumber. The magnetic field spectral PW components are given by

$$\begin{aligned}\check{H}_y^i(\mathbf{r}, \omega; \kappa_y) &= \frac{I_0 \omega n'_1 \sqrt{\alpha}}{2c} \exp[-j\omega \tilde{\tau}^i(\kappa_y)] \\ \check{H}_z^i(\mathbf{r}, \omega; \kappa_y) &= \frac{-I_0 \omega n'_1 \alpha \kappa_y}{2c \kappa_z} \exp[-j\omega \tilde{\tau}^i(\kappa_y)].\end{aligned}\quad (15)$$

Recall that over tilde ($\check{}$) denotes PW constituents. The integration contour is in the upper Riemann sheet where $\text{Re} \kappa_z \geq 0$. Note that in the fields' representation in (9)–(14), we have recast the spectral representation in [22] and, anticipating the extension to the time domain, utilized the normalized (with respect to ω) spectral wavenumber $\kappa_y = k_y c / (\sqrt{\alpha} n'_1 \omega)$.

The TD PW representation of the incident field is obtained by substituting (10) with either (11) or (15) into (9). By inverting the order of integrations and evaluating the $d\omega$ integration

in closed form, we obtain the TD spectral representation of the analytic field in the form

$$\begin{aligned}\check{E}_x^i(\mathbf{r}, t) &= \frac{\partial_t}{2\pi j} \int d\kappa_y \check{E}_x^i(\mathbf{r}, t; \kappa_y) \\ \check{H}_{y,z}^i(\mathbf{r}, t) &= \frac{\partial_t}{2\pi j} \int d\kappa_y \check{H}_{y,z}^i(\mathbf{r}, t; \kappa_y)\end{aligned}\quad (16)$$

where

$$\begin{aligned}\check{E}_x^i(\mathbf{r}, t; \kappa_y) &= -\frac{I_0 \mu'_1 \sqrt{\alpha}}{2\kappa_z} \check{\delta}[t - \tilde{\tau}^i(\kappa_y)] \\ \check{H}_y^i(\mathbf{r}, t; \kappa_y) &= \frac{I_0 n'_1 \sqrt{\alpha}}{2c} \check{\delta}[t - \tilde{\tau}^i(\kappa_y)] \\ \check{H}_z^i(\mathbf{r}, t; \kappa_y) &= \frac{I_0 n'_1 \alpha \kappa_y}{2c \kappa_z} \check{\delta}[t - \tilde{\tau}^i(\kappa_y)]\end{aligned}\quad (17)$$

are the TD PWs. In (17), $\check{\delta}()$ denotes the analytic delta function

$$\check{\delta}(t) = \begin{cases} (-\pi j t)^{-1}, & \text{Im } t < 0 \\ \delta(t) + j \mathcal{P}(\pi t)^{-1}, & \text{Im } t = 0 \end{cases} \quad (18)$$

where \mathcal{P} denotes Cauchy's principal value.

B. Reflected Field

The boundary problem at hand is solved by transforming each spectral incident PW in (11) and (15) to the *medium frame* where the medium's planar discontinuity is stationary. Each PW in the source frame is transformed into a PW in the medium frame with a corresponding frequency and wavenumber. The scattering of each PW in the comoving frame is treated in a classical way. Finally, the scattered fields are transformed back to the *source frame* obtaining the corresponding TD PW spectral representations. Here we use the TH spectral representation of the reflected fields in [23, eqs. (37)–(39)] and follow essentially the same procedure as for the incident field in (16) and (17).

The resulting spectral integrals of the EM reflected fields are of the integral form of (16) over the reflected spectral PWs

$$\begin{aligned}\check{E}_x^r(\mathbf{r}, t; \kappa_y) &= \frac{-I_0 \mu'_1 \tilde{\Gamma}'(\kappa_y)}{2\kappa_z \sqrt{\alpha} \gamma^2 (\tilde{\xi} - n'_1 \beta \tilde{\zeta})} \check{\delta}[t - \tilde{\tau}^r(\kappa_y)] \\ \check{H}_y^r(\mathbf{r}, t; \kappa_y) &= \frac{1}{-\eta'_1 \gamma \tilde{\xi} - 2n'_1 \beta \kappa_z} \tilde{\xi} - n'_1 \beta \tilde{\zeta} \check{E}_x^r(\mathbf{r}, t; \kappa_y) \\ \check{H}_z^r(\mathbf{r}, t; \kappa_y) &= \frac{-\kappa_y}{\eta'_1 \gamma \sqrt{\alpha} \gamma^2 \tilde{\xi}^2} \check{E}_x^r(\mathbf{r}, t; \kappa_y)\end{aligned}\quad (19)$$

where $\eta'_1 = \sqrt{\mu'_1/\epsilon'_1}$, and $\tilde{\xi}$ and $\tilde{\zeta}$ are given by

$$\tilde{\xi} = 1 - n'_1 \beta \kappa_z, \quad \tilde{\zeta} = \kappa_z - n'_1 \beta. \quad (20)$$

In (19), the spectral delay is given by

$$\tilde{\tau}^r(\kappa_y) = \frac{n'_1/c}{\tilde{\xi} - n'_1 \beta \tilde{\zeta}} \left[\frac{\kappa_y}{\sqrt{\alpha} \gamma^2} y + \frac{\beta}{n'_1} \tilde{\xi} z + \tilde{\zeta} (2z_0 - z) \right] \quad (21)$$

and

$$\tilde{\Gamma}'(\kappa_y) = \frac{\mu'_2 \tilde{\zeta} - \mu'_1 \sqrt{n_{21}^2 \tilde{\xi}^2 - \kappa_y^2 / (\alpha \gamma^2)}}{\mu'_2 \tilde{\xi} + \mu'_1 \sqrt{n_{21}^2 \tilde{\xi}^2 - \kappa_y^2 / (\alpha \gamma^2)}}, \quad n'_{21} = n'_2/n'_1 \quad (22)$$

is the (medium-frame) reflection coefficient at the interface.

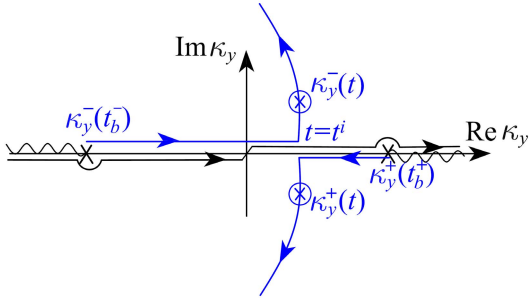


Fig. 2. Integration contour and the complex poles in the complex κ_y plane. Here $\text{Re}\kappa_z > 0$ on entire top Riemann sheet and $\text{Im}\kappa_z \leq 0$ in the first and third quadrants.

III. STT DERIVATION OF THE EXACT FIELDS

In this section, we evaluate the TD PW spectral integrals of the incident and reflected EM fields in closed form *directly in the source frame* by applying the STT. Recall that in the source frame, the planar interface is moving, and thus each scattered spectral PW exhibits a different frequency and wavenumber. Even the concept of TH $\exp(j\omega t)$ fields cannot in general be applied to here. Though the STT was aimed at obtaining a method that evaluates TH spectral integrals, in this section, we demonstrate its ability to handle a problem of *time-variant* type scattering.

A. Incident Field

1) *Spectral Properties*: We distinguish two spectral intervals: 1) the *propagating* (or visible) spectrum, $|\kappa_y| < 1$, where κ_z in (14) and therefore the spectral delay in (12) are real and 2) the *evanescent* (or invisible) spectrum, $|\kappa_y| > 1$, where κ_z is imaginary. In the evanescent spectral range, $\tilde{\tau}^i$ is complex and the local TD PWs decay.

In order to evaluate the incident field $\check{\mathbf{E}}^i(\mathbf{r}, t)$, we recast the spectral integral of the incident field in (16) in the canonical STT form of (8)

$$\check{E}_x^i(\mathbf{r}, t) = \frac{\partial_t}{2\pi^2} \int_{-\infty}^{\infty} d\kappa_y \frac{\check{A}^i(\kappa_y)}{t - \tilde{\tau}^i(\kappa_y)} \quad (23)$$

where $\tilde{\tau}^i(\kappa_y)$ is given in (12) and the amplitude

$$\check{A}^i(\mathbf{r}, t) = -I_0 \mu_1' \sqrt{\alpha} / 2\kappa_z. \quad (24)$$

The branch points are $\kappa_{yb} = \pm 1$ and the integration contour is plotted in Fig. 2.

Next, following the STT procedure, we solve the equation $\tilde{\tau}^i[\kappa_y^\pm(t)] = t$ and obtain the TD poles in the complex κ_y -plane. By using $\tilde{\tau}^i$ in (12), we obtain the two poles

$$\kappa_y^\pm(t) = \frac{yZ_1^i \pm Z_2^i \sqrt{\alpha(y^2 + Z_2^i{}^2 - Z_1^i{}^2)}}{\sqrt{\alpha}(y^2 + Z_2^i{}^2)} \quad (25)$$

where

$$Z_1^i = (mz + ct)/n_1', \quad Z_2^i = \sqrt{\alpha}z. \quad (26)$$

In (25), we choose $\text{Im}\sqrt{\cdot} \leq 0$.

Next we map the poles trajectories in time over the complex κ_y upper Riemann sheet. Prior to $ct_b^\pm = (-mz \pm yn_1'\sqrt{\alpha})$,

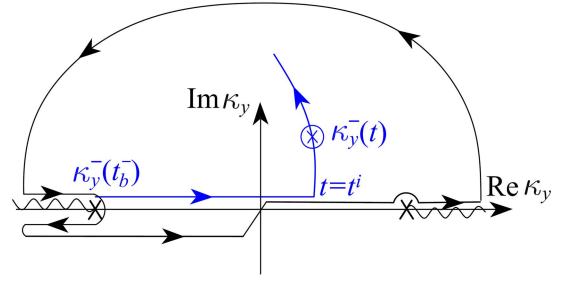


Fig. 3. Integration contour in complex κ_y -plane.

the κ_y^\pm poles travel on the *lower* Riemann sheet, respectively. At $t = t_b^\pm$, the κ_y^\pm poles enter the *upper* Riemann sheet at $\kappa_b = \pm 1$, respectively, after which they move toward each other over the real κ_y -axis. At time

$$ct^i = -mz + \sqrt{\alpha}R^i n_1', \quad R^i = \sqrt{y^2 + \alpha z^2} \quad (27)$$

both poles reach $\kappa_y^i = y/(\sqrt{\alpha}R^i)$ over the real (visible spectrum) axis. At the time interval $t > t^i$, the term $y^2 + Z_2^i{}^2 - Z_1^i{}^2$ in (25) is negative, and the poles depart from the real axis along the trajectories in Fig. 2.

2) *Integral Evaluation*: Following the STT procedure in [15], we close the integration contour as in Fig. 3. Thus, the spectral integral in (23) can be evaluated in closed form via the contribution of κ_y^- pole (see [16])

$$\check{E}_x^i(\mathbf{r}, t) = \frac{j}{\pi} \check{A}^i(\kappa_y) / \dot{\tilde{\tau}}^i(\kappa_y^-) \quad (28)$$

where κ_y^- is given in (25) and the over dot denotes a derivative with respect to the argument. The derivative of the spectral delay $\tilde{\tau}^i(\kappa_y)$ in (12) is

$$\dot{\tilde{\tau}}^i(\kappa_y) = \sqrt{\alpha}(\kappa_z y - \sqrt{\alpha}\kappa_y z) / \kappa_z v_1'. \quad (29)$$

By substituting (29) into (28) and taking the real part (note that the spectral amplitude is real in the visible spectrum), we obtain the TD physical field in the form

$$E_x^i(\mathbf{r}, t) = \partial_t \text{Im} \left[-\frac{1}{2\pi} \frac{I_0 \mu_1' v_1'}{y\kappa_z - \sqrt{\alpha}z\kappa_y} \right] \Big|_{\kappa_y = \kappa_y^-(t)}. \quad (30)$$

Note that $\check{A}^i(\kappa_y) / \dot{\tilde{\tau}}^i(\kappa_y^-)$ is imaginary for $t < t^i$, and therefore the real physical field is null in this time interval. By substituting κ_y^- in (25) into (30), we obtain

$$E_x^i(\mathbf{r}, t) = -\frac{I_0 \mu_1'}{2\pi} H(t - t^i) / \sqrt{(t + mz/c)^2 - (t^i + mz/c)^2} \quad (31)$$

where $H()$ denotes the Heaviside step function. This result is in accordance with the one in [24]. Also, note that by setting $\beta = 0$ in (31), we obtain the (stationary-medium) conventional 2-D TD Green's function.

By using (31), t^i is identified as the incident wavefront travel time from the source to the observer in the source frame. This travel time differs from the stationary medium one which equals $(y^2 + z^2)^{1/2}/v_1'$ in two ways: 1) the $-mz/c$ term that increases the speed in the direction of the medium motion and 2) the term $\sqrt{\alpha}z$ that is due to special relativity space contraction in the direction of the movement.

B. Reflected Wave

1) *Spectral Properties*: In order to evaluate the reflected field in closed form, we recast its spectral representation in the standard STT form

$$\check{E}_x^r(\mathbf{r}, t) = \frac{\partial_t}{2\pi^2} \int_{-\infty}^{\infty} d\kappa_y \frac{\check{A}^r(\kappa_y)}{t - \check{\tau}^r(\kappa_y)} \quad (32)$$

where $\check{\tau}^r(\kappa_y)$ is given in (21) and the amplitude

$$\check{A}^r(\kappa_y) = \frac{-I_0 \mu'_1}{2\kappa_z \sqrt{\alpha} \gamma^2 (\check{\xi}^- - n'_1 \beta \check{\zeta}^-)} \check{\Gamma}'(\kappa_y). \quad (33)$$

The reflection coefficient $\check{\Gamma}'(\kappa_y)$ in (22) gives rise to two additional branch points

$$\kappa_{yb}^{\pm} = \pm \sin \theta'_c / [\sqrt{\alpha} \gamma (1 + n'_1 \beta \cos \theta'_c)] \quad (34)$$

where

$$\sin \theta'_c = n_{2,1} \quad (35)$$

is identified as the stationary interface critical angle.

Next, following the STT procedure, we solve the equation $\check{\tau}^r[\kappa_y^{\pm}(t)] = t$ and obtain the reflected field TD poles in the complex κ_y -plane. By using $\check{\tau}^r$ in (21), these TD poles are

$$\kappa_y^{\pm}(t) = \frac{y Z'_1 \pm Z'_2 \sqrt{y^2 + Z'_2{}^2 - Z'_1{}^2}}{y^2 + Z'_2{}^2} \quad (36)$$

where

$$\begin{aligned} Z'_1 &= \sqrt{\alpha} \gamma^2 [n'_1 \beta (2z_0 - z + \beta ct) + (ct - \beta z)/n'_1] \\ Z'_2 &= \sqrt{\alpha} \gamma^2 (2z_0 - z - \beta^2 z + 2\beta ct). \end{aligned} \quad (37)$$

As in (25), we choose $\text{Im} \sqrt{\cdot} \leq 0$.

Next we map the poles trajectories in time over the complex κ_y upper Riemann sheet. Prior to

$$ct_b^{\pm} = mz - \left[\frac{2n_1'^2 \beta (z - z_0) \mp n_1' y / \sqrt{\alpha} \gamma^2}{1 - n_1'^2 \beta^2} \right] \quad (38)$$

the κ_y^{\pm} poles lie on the *lower* Riemann sheet, respectively. At $t = t_b^{\pm}$, the κ_y^{\pm} poles enter the upper Riemann sheet at $\kappa_b = \pm 1$, after which they move toward each other over the real κ_y -axis. Over the real (visible spectrum) axis, the poles converge to

$$\kappa_y^+ = \kappa_y^- = y/Z'_1|_{t=t^r} \quad (39)$$

at time

$$\begin{aligned} ct^r &= \frac{A + \sqrt{n_1'^2 (2Z_0 - z + \beta^2 z)^2 + Y^2}}{1 - n_1'^2 \beta^2} \\ A &= \beta [z + n_1'^2 (2z_0 - z)], \quad Y = n_1' y / \sqrt{\alpha} \gamma^2. \end{aligned} \quad (40)$$

At the time interval $t > t^r$, the term $y^2 + Z_2'^2 - Z_1'^2$ in (36) is negative, and the poles depart from the real axis along the trajectories in Fig. 2.

2) *Integral Evaluation for $n'_{21} > 1$* : Following the STT procedure in [15], we close the integration contour as in Fig. 3 and evaluate the spectral integral in (32) in closed form via the contribution of κ_y^- pole in (36). This procedure yields

$$E_x^r(\mathbf{r}, t) = \text{Re} \left[\frac{j}{\pi} \check{A}^r(\kappa_y^-) / \check{\tau}^r(\kappa_y^-) \right] \quad (41)$$

where \check{A}^r is given in (33). By using $\check{\tau}^r$ in (21), we evaluate

$$\begin{aligned} \check{\tau}^r(\kappa_y) &= \frac{n'_1}{c \kappa_z \alpha \gamma^2 (\check{\xi}^- - n'_1 \beta \check{\zeta}^-)^2} \\ &\times \left\{ y \sqrt{\alpha} [\kappa_z (1 + n_1'^2 \beta^2) - 2n_1' \beta] - \kappa_y (2z_0 - \gamma^{-2} z) \right\}. \end{aligned} \quad (42)$$

Following the discussion after (37), we identify different pole contributions to the field according to the value of $n'_{21} = n'_2/n'_1$. For $n'_{21} > 1$, the reflection coefficient $\check{\Gamma}'(\kappa_y)$ is real over the entire visible spectral range. Therefore, the spectral amplitude, \check{A}^r , in (33) is real over the time interval $t < t^r$ and the reflected field in (32) is null.

For $t > t^r$, the pole κ_y^- in (36) is complex and therefore so are the corresponding κ_z and $\check{\Gamma}'(\kappa_y)$ in (14) and (22). By substituting (33) and (42) into (41), we obtain

$$\begin{aligned} E_x^r(\mathbf{r}, t) &= \frac{I_0 \mu'_1 c \sqrt{\alpha}}{2\pi n'_1} H(t - t^r) \\ &\times \text{Im} \left[\frac{(\check{\xi}^- - n'_1 \beta \check{\zeta}^-) \check{\Gamma}'(\kappa_y^-)}{y \sqrt{\alpha} [\kappa_z^- (1 + n_1'^2 \beta^2) - 2n_1' \beta] - \kappa_y^- (2z_0 - \gamma^{-2} z)} \right] \end{aligned} \quad (43)$$

where κ_y^- is given in (36), t^r is given in (40), and $\check{\xi}^- = \check{\xi}(\kappa_y^-)$ and $\check{\zeta}^- = \check{\zeta}(\kappa_y^-)$ are given in (20). Note that by substituting $\beta = 0$ in (43), we obtain the for stationary medium reflected field in [16].

In order to gain insight into the result in (43), we consider the special case of the on-axis $y = 0$ field. The *incident* wave wavefront is given by $ct = ct^i$ where ct^i is given in (27). By setting $y = 0$, this wavefront is given by $ct^i(z) = -mz + an'_1 |z|$. Thus, we distinguish two wave speed, $v^{\pm} = c/(an'_1 \mp m)$, in the direction of $\pm z$, respectively. This anisotropy is due to the medium's movement in the direction of the z -axis that increases or decreases the wave speed propagating in the direction of or opposite the medium velocity.

Using these wave velocities, we recast the (z -axis) reflected wavefront arrival time in (40) as the sum $ct^r = ct_i^r + ct_r^r$ where we define

$$ct_i^r = (z_0 + vt_i^r)/v^+, \quad ct_r^r = (z_0 - z + vt_r^r)/v^-. \quad (44)$$

Thus, we identified t_i^r as the time required for the *incident* wavefront (that is propagating with v^+ speed) to reach the interface that is located at $z_0 + vt_i^r$. After that, the *reflected* wavefront is propagating for t_r^r with speed of v^- toward the observation point a distance of $z_0 - z + vt_r^r$ and arriving at z at time t^r . This interpretation can be generalized for off-axis observation points along the reflected wavefront.

The total TD field $E_x^i(\mathbf{r}, t) + E_x^r(\mathbf{r}, t)$ in (31) and (43) is plotted in Fig. 4 for $z_0 = 1$, $n'_1 = 1.2$, $n'_2 = 1.5$, $\mu'_1 = \mu'_2 = 1$, and $I_0 = 1$ and $\beta = 0.65$. The fields that are sampled at

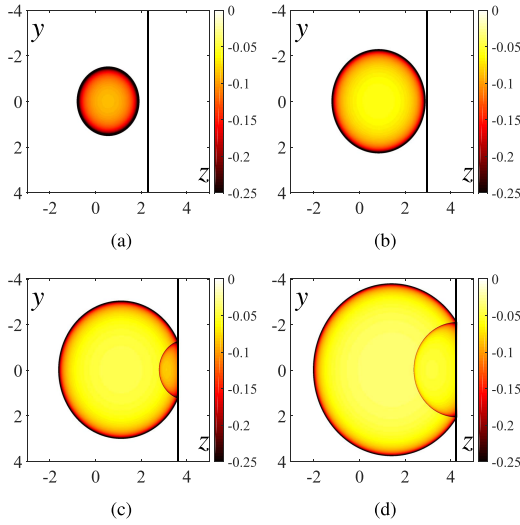


Fig. 4. Total TD field for $n'_1 = 1.2$ and $n'_2 = 1.5$. Here $z_0 = 1$, $\beta = 0.65$, $\mu'_1 = \mu'_2 = 1$, and $I_0 = 1$. (a)–(d) Fields that are sampled for $ct = 2, 3, 4$, and 5 , respectively.

$ct = 2, 3, 4$, and 5 are plotted in Fig. 4(a)–(d), respectively. For these parameters, $n'_{21} > 1$, so no head wave is present in Fig. 4(a)–(d).

3) *Integral Evaluation for $n'_{21} < 1$* : In the case of $n'_{21} < 1$, the branch cuts due to the square root in the reflection coefficient in (22) are extending from κ_{yb}^\pm in (34) to $\pm\infty$, respectively. The κ_y^- pole is arriving at the brunch point κ_{yb}^+ at time $t_b = \tilde{\tau}^r(\kappa_{yb})$. By using $\tilde{\tau}^r$ in (21) and κ_{yb}^+ in (34), we obtain

$$ct_b = \frac{n'_1}{\tilde{\zeta}_b - n'_1\beta\tilde{\zeta}_b} \left[\frac{\cos\tilde{\varphi}_b}{\sqrt{\alpha}\gamma^2} y + \frac{\beta}{n'_1}\tilde{\zeta}_b z + \tilde{\zeta}_b(2z_0 - z) \right] \quad (45)$$

where

$$\tilde{\zeta}_b = 1 - n'_1\beta \cos\tilde{\varphi}_b, \quad \tilde{\zeta}_b = \cos\tilde{\varphi}_b - n'_1\beta. \quad (46)$$

Here $\tilde{\varphi}_b$ is the branch cut angle $\sin\tilde{\varphi}_b = \kappa_{yb}^+$.

Thus, in the time interval $t_b < t < t^r$, the TD pole κ_y^- is moving along the real visible axis along the interval $\kappa_{yb} < \kappa_y < \kappa_{y0}$. At this time interval, the reflection coefficient is complex and its imaginary part contribution to the field in (41) gives rise to the lateral (head) wave. In the time interval $t > t^r$, the TD pole κ_y^- is complex as well as the reflection coefficient.

By substituting (36) into (41) and using (42), we obtain the result for $t_b < t < t^r$

$$E_x^r(\mathbf{r}, t) = \frac{I_0\mu'_1 c\sqrt{\alpha}}{2\pi n'_1} \times \frac{(\tilde{\zeta}_b^- - n'_1\beta\tilde{\zeta}_b^-)\text{Im}\tilde{\Gamma}'(\kappa_y^-)}{y\sqrt{\alpha}[\kappa_y^-(1 + n_1'^2\beta^2) - 2n_1'\beta] - \kappa_y^-(2z_0 - \gamma^{-2}z)}. \quad (47)$$

The reflected and lateral wave contributions in the time interval $t > t^r$ are given by (43). Note that by setting $\beta = 0$ in (47), we obtain the stationary medium lateral wave in [16].

In order to gain insight into the (dynamic scattering) lateral wave, we recast the lateral wave time of arrival, ct_b , in (45) in the form

$$ct_b = ct_b^i + ct_b^l + ct_b^r \quad (48)$$

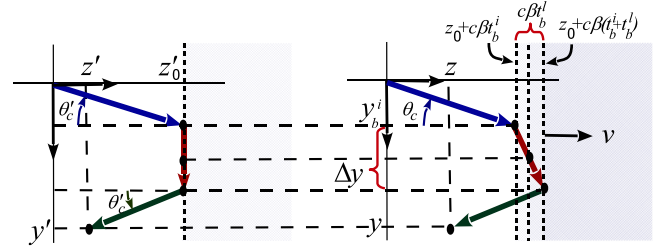


Fig. 5. Interpretation of the lateral wave in the (left) medium and (right) source frames. The source-frame excitation event $(y, z, ct) = (y_b^i, z_b^i = z_0 + \beta ct_b^i, ct_b^i)$ on the right is corresponding to the medium-frame event (on the left) in which the incident wavefront is impinging upon the interface at the critical angle θ'_c . The radiation event $(y, z, ct) = (y_b^l + \Delta y, z_0 + \beta c(t_b^l + t_b^i), ct_b^l + ct_b^i)$ in the source frame on the right is corresponding to the medium-frame event in which the wavefront emanates from the interface. The medium-frame horizontal lateral propagation is mapped to a tilted (red) line in the source frame along the moving interface.

where we define

$$\begin{aligned} ct_b^i &= \gamma^2 z_0 (\beta + n'_1 / \cos\theta'_c) \\ ct_b^l &= \gamma n'_2 \Delta y, \\ ct_b^r &= \gamma \left(\frac{y - \Delta y}{\sin\theta'_c} - \frac{\gamma z_0}{\cos\theta'_c} \right) (n'_1 - \beta \cos\theta'_c) \end{aligned} \quad (49)$$

with

$$\Delta y = \frac{y(\beta n'_1 - \cos\theta'_c) + \sin\theta'_c(2\gamma z_0 - z/\gamma)}{\cos\theta'_c(\beta n'_1 \cos\theta'_c - 1)}. \quad (50)$$

This representation identifies three events along the lateral wavefront that are marked in Fig 5. The first event $(y, z, ct) = (y_b^i, z_b^i, ct_b^i)$ is the *excitation* of the lateral wave where $y_b^i = z_0\gamma \tan\theta'_c$, $z_b^i = z_0 + \beta ct_b^i$, and t_b^i is given in (49). By using the LT in (1), we note that this event in the medium frame is corresponding to the conventional (stationary interface) event in which the incident wavefront is impinging upon the interface at the critical angle θ'_c (see Fig. 5).

The second event is the *radiation* event $(y, z, ct) = (y_b^l + \Delta y, z_b^l, ct_b^l + ct_b^i)$ in which the lateral wavefront emanates from the interface back to medium 1. Here $z_b^l = z_0 + \beta c(t_b^l + t_b^i)$ is located over the moving interface. Thus, we identified t_b^l as the lateral propagation time along the moving interface. In the *medium frame*, the wave is propagating along the interface in the direction of the y' -axis at the medium-frame speed of c/n'_2 . In the *source frame*, the lateral trajectory is tilted with respect to the interface due to its movement (see Fig. 5). The third event is the arrival of the wavefront to the observation event $(y, z, ct) = (y, z, ct_b)$. The wave is propagating in the moving medium 1 for ct_b after emanating from the interface at $ct_b^l + ct_b^i$.

Finally, we evaluate the source-frame critical angle, θ_c , in which the lateral wave is excited (see Fig. 5). The incident wavefront is given by (27) where t^i is a parameter. The normal vector to this wavefront is obtained by taking the gradient of the right-hand side of (27). By normalizing the resulting normal, sampling at the excitation event $(y, z, ct) = (y_b^i, z_b^i, ct_b^i)$,

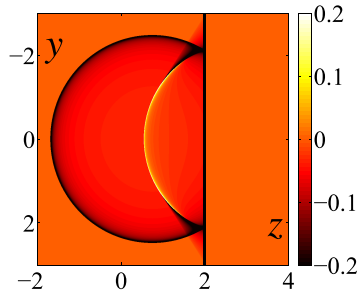


Fig. 6. Total fields for $n'_1 = 2$, $n'_2 = 1$, $\beta = 0.2$, and $ct = 5$. Here $n'_2 < n'_1$ and a lateral wave is excited.

and projecting on the y -axis, we obtain

$$\sin \theta_c = \frac{\chi}{\sqrt{[\alpha^2 n_1'^2 (1 + \beta c \bar{t}_b^i) - m^2 - m c \bar{t}_b^i (1 + \beta m)]^2 + \chi^2}},$$

$$\chi = \alpha n_1'^2 \gamma \tan \theta'_c, \quad c \bar{t}_b^i = \gamma^2 (\beta + n_1'^2 \tan \theta'_c) \quad (51)$$

where θ'_c is given in (35). Note that the critical angle is $(\beta -)$ speed dependent and that by setting $\beta = 0$ in (51), we obtain $\sin \theta_c = \sin \theta'_c$.

In Fig. 6, the source-frame exact solutions for the incident and reflected fields are plotted for medium parameters: $n'_1 = 2$, $n'_2 = 1$, and $\beta = 0.2$ and the fields are sampled at $ct = 5$. All other parameters are the same as in Fig. 4. Here $n'_2 < n'_1$ and the lateral wave is excited and clearly viewed in Fig. 6.

IV. CONCLUSION

In this paper, the TD incident and reflected fields of a TD line current that is embedded in a moving dielectric-magnetic medium with a planar discontinuity were obtained in closed form by applying the STT procedure. The unique scattering mechanism of the TD lateral (head) wave was analyzed and put in a noble canonical form identifying the excitation mechanism, lateral propagation form along the moving interface, and the back radiation toward the observation point. The investigation reveals basic wave phenomena relating to a canonical problem, and on route demonstrated the ability of the STT to handle a new class of problems.

REFERENCES

- [1] T. B. Hansen and A. Yaghjian, *Plane-Wave Theory of Time-Domain Fields: Near-Field Scanning Applications*. New York, NY, USA: Wiley, 1999.
- [2] S. L. Dvorak, R. W. Ziolkowski, and L. B. Felsen, "Hybrid analytical-numerical approach for modeling transient wave propagation in Lorentz media," *J. Opt. Soc. Amer. A, Opt. Image Sci.*, vol. 15, no. 5, pp. 1241–1255, 1998.
- [3] T. Melamed and L. B. Felsen, "Pulsed-beam propagation in dispersive media via pulsed plane wave spectral decomposition," *IEEE Trans. Antennas Propag.*, vol. 48, no. 6, pp. 901–908, Jun. 2000.
- [4] E. Heyman, "Time-dependent plane-wave spectrum representations for radiation from volume source distributions," *J. Math. Phys.*, vol. 37, no. 2, pp. 658–681, 1996.
- [5] A. Shlivinski, E. Heyman, and R. Kastner, "Antenna characterization in the time domain," *IEEE Trans. Antennas Propag.*, vol. 45, no. 7, pp. 1140–1149, Jul. 1997.
- [6] A. Shlivinski, E. Heyman, and A. J. Devaney, "Time domain radiation by scalar sources: Plane wave to multipole transform," *J. Math. Phys.*, vol. 42, pp. 5915–5919, Nov. 2001.
- [7] E. A. Marengo and A. J. Devaney, "Time-dependent plane wave and multipole expansions of the electromagnetic field," *J. Math. Phys.*, vol. 39, pp. 3643–3660, Jun. 1998.

- [8] T. Melamed, "Pulsed beam expansion of electromagnetic aperture fields," *Prog. Electromagn. Res.*, vol. 114, pp. 317–332, 2011.
- [9] T. Melamed, D. Abuhasira, and D. Dayan, "Transverse electric and transverse magnetic pulsed beam decomposition of time-dependent aperture fields," *J. Opt. Soc. Amer. A, Opt. Image Sci.*, vol. 29, no. 6, pp. 1115–1123, 2012.
- [10] T. Melamed, Y. Ehrlich, and E. Heyman, "Short-pulse inversion of inhomogeneous media: A time-domain diffraction tomography," *Inverse Problems*, vol. 12, no. 6, pp. 977–993, 1996.
- [11] Y. Hadad and T. Melamed, "Time-dependent tilted pulsed-beams and their properties," *IEEE Trans. Antennas Propag.*, vol. 59, no. 10, pp. 3855–3862, Oct. 2011.
- [12] I. Tinkelman and T. Melamed, "Local spectrum analysis of field propagation in an anisotropic medium. Part II. Time-dependent fields," *J. Opt. Soc. Amer. A, Opt. Image Sci.*, vol. 22, no. 6, pp. 1208–1215, 2005.
- [13] R. Tuvi and T. Melamed, "Scalar pulsed beam scattering by a fast moving soft wedge," in *Proc. URSI Gen. Assembly Sci. Symp.*, Aug. 2014, pp. 1–4.
- [14] E. Heyman and L. Felsen, "Weakly dispersive spectral theory of transients, part I: Formulation and interpretation," *IEEE Trans. Antennas Propag.*, vol. AP-35, no. 1, pp. 80–86, Jan. 1987.
- [15] E. Heyman and L. Felsen, "Weakly dispersive spectral theory of transients (STT), part II: Evaluation of the spectral integral," *IEEE Trans. Antennas Propag.*, vol. AP-35, no. 5, pp. 574–580, May 1987.
- [16] E. Heyman, "Weakly dispersive spectral theory of transients, part III: Applications," *IEEE Trans. Antennas Propag.*, vol. AP-35, no. 11, pp. 1258–1266, Nov. 1987.
- [17] E. Heyman, R. Strachievlevitz, and D. Kosloff, "Pulsed beam reflection and transmission at a planar interface: Exact solutions and approximate local models," *Wave Motion*, vol. 18, no. 4, pp. 315–343, 1993.
- [18] R. Iaconescu and E. Heyman, "Pulsed field diffraction by a perfectly conducting wedge: A spectral theory of transients analysis," *IEEE Trans. Antennas Propag.*, vol. 42, no. 6, pp. 781–789, Jun. 1994.
- [19] B. de Hon, E. Heyman, and L. Felsen, "Spectral alternatives for the synthesis of short-pulse wavefields in waveguides," in *Proc. Ultra-Wideband Short-Pulse Electromagn.*, vol. 4. New York, NY, USA, 1999, pp. 289–299.
- [20] E. Heyman and B. Z. Steinberg, "Spectral analysis of complex-source pulsed beams," *J. Opt. Soc. Amer. A, Opt. Image Sci.*, vol. 4, no. 3, pp. 473–480, 1987.
- [21] Y. Kaganovsky and E. Heyman, "Spectral analysis of the airy pulsed beam," in *Proc. 30th URSI Gen. Assembly Sci. Symp.*, Piscataway, NJ, USA, Aug. 2011, p. 4.
- [22] T. Danov and T. Melamed, "Spectral analysis of relativistic dyadic Green's function of a moving dielectric-magnetic medium," *IEEE Trans. Antennas Propag.*, vol. 59, no. 8, pp. 2973–2979, Aug. 2011.
- [23] T. Danov and T. Melamed, "Two-dimensional relativistic longitudinal Green's function in the presence of a moving planar dielectric-magnetic discontinuity," *J. Opt. Soc. Amer. A, Opt. Image Sci.*, vol. 29, no. 3, pp. 285–294, 2011.
- [24] T. Danov and T. Melamed, "A simple and direct time domain derivation of the dyadic Green's function for a uniformly moving non-dispersive dielectric-magnetic medium," *IEEE Trans. Antennas Propag.*, vol. 60, no. 5, pp. 2594–2597, May 2012.

Timor Melamed (SM'94) was born in Tel-Aviv, Israel, in 1964. He received the B.Sc. degree (*magna cum laude*) in electrical engineering and the Ph.D. degree from Tel-Aviv University, Tel-Aviv, in 1989 and 1997, respectively.

From 1996 to 1998, he held a post-doctoral position at the Department of Aerospace and Mechanical Engineering, Boston University, Boston, MA, USA. He is currently with the Department of Electrical and Computer Engineering, Ben-Gurion University of the Negev, Beer Sheva, Israel. He is a beau of SLG, Holon, Israel. His current research interests include analytic techniques in wave theory, transient wave phenomena, inverse scattering, and electrodynamics.

Tatiana Danov was born in Rubtsovsk, Russia, in 1966. She received the M.Sc. degree (*magna cum laude*) in physics from Lobachevsky University, Gorky, Russia, in 1988, and the Ph.D. degree in electrical engineering from the Ben-Gurion University of the Negev, Beer Sheva, Israel, in 2014.

From 1989 to 2000, she was with the Department of Physics and Electrical Engineering, Technical University in Nizhny Novgorod, Nizhny Novgorod, Russia. From 2002 to 2006, she was with the VLSI Center, Ben-Gurion University of the Negev.